Journal Pre-proof

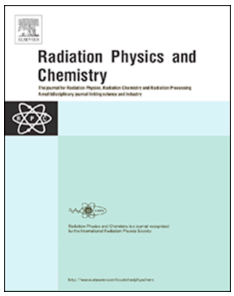

Spectroscopic properties of the gamma irradiated ErF_3-DOPED BaF_2 crystals

Marius Stef, Irina Nicoara, Andrei Racu, Gabriel Buse, Daniel Vizman

PII: S0969-806X(20)30195-X

DOI: https://doi.org/10.1016/j.radphyschem.2020.109024

Reference: RPC 109024

To appear in: *Radiation Physics and Chemistry*

Received Date: 21 February 2020

Revised Date: 8 May 2020

Accepted Date: 5 June 2020

Please cite this article as: Stef, M., Nicoara, I., Racu, A., Buse, G., Vizman, D., Spectroscopic properties of the gamma irradiated ErF_3-DOPED BaF_2 crystals, *Radiation Physics and Chemistry* (2020), doi: https://doi.org/10.1016/j.radphyschem.2020.109024.

Marius Stef: Conceptualization, Methodology, Software, Formal analysis, Investigation, Writing - Original Draft , Writing- Reviewing and Editing, **Irina Nicoara.**: Formal analysis, Writing- Reviewing and Editing, Supervision. **Andrei Racu**: Investigation, Formal analysis, . **Gabriel Buse***:* Formal analysis, Investigation, Writing - Review & Editing, **Daniel Vizman**: Resources, Funding acquisition.

SPECTROSCOPIC PROPERTIES OF THE GAMMA IRRADIATED ErF_3-DOPED BaF_2 CRYSTALS

Marius Stef[a,*], Irina Nicoara[a], Andrei Racu[b], Gabriel Buse[a] and Daniel Vizman[a]

[a]*West University of Timisoara, 4 Bd.V. Parvan, Timisoara* 300223, *Romania*

[b]*National Institute of Research & Development for Electrochemistry and Condensed Matter – INCEMC Timisoara, 144 Dr. Aurel Păunescu-Podeanu, RO-300569 Timisoara, Romania*

Corresponding author: marius.stef@e-uvt.ro

Keywords: barium fluoride crystal; gamma rays irradiation; optical properties; Judd-Ofelt analysis; luminescence

Abstract

The spectroscopic properties of the gamma irradiated $BaF_2:Er^{3+}$ crystals were studied. BaF_2:0.2 mol% ErF_3 crystal was grown using the vertical Bridgman method. The Judd-Ofelt intensity parameters, Ω_t (t=2,4,6) for *f-f* transitions of Er^{3+} ions were determined from optical absorption spectra recorded before and after gamma irradiation at various doses. The influence of gamma irradiation dose on the Judd-Ofelt parameters and on the radiative transition probability, on the branching ration and on the radiative lifetime was also investigated. The predicted radiative lifetimes were compared with those measured and with those reported by other authors. Apart from the green and red emissions, arising under excitation at 378 nm, a new UV emission band around 321 nm was observed under excitation at 290 nm. This emission was not reported before. Using the Füchtbauer-Ladenburg method, the emission cross section and optical gain parameter of the red and green emission band were calculated.

1. Introduction

In the last time, trivalent rare-earth (RE) ions doped fluoride MeF_2 (Me=Ca, Sr, Ba) crystals have been extensively investigated. Due to their optical properties, such as low phonon energy, broadband transmission over a wide spectral range from ultraviolet to far-infrared (200-14.000 nm), large bandgap energies, low spectral dispersion and relatively low refractive index, the MeF_2 crystals have been studied for various applications (optical windows, lenses, optical communications, laser host materials, scintilators, etc.) (Hahn, 2014). In BaF_2 crystals containing various RE ions, only trigonal spectra were detected by (Wells et al., 2002; Ranon and Yaniv,1964; Petit et al., 2007; Nicoara et al., 2016). They attributed these spectra to sites where F^- ions occupy interstitial body centers of next-nearest cubes along the [111] direction, the so-called *NNN* sites.

The choice of host materials is of great importance in the designing of RE doped luminescent materials for various practical applications. Fluorides are considered good hosts for upconversion luminescence of RE^{3+} ions. The emission spectrum of Tb^{3+}-doped BaF_2 consists of two sets of lines, so-called the blue and the green emission (Witkowski and Wojtowicz, 2011)**.** Orlovskii et al., (Orlovskii et al. 2010) studied the double doped BaF_2:Tm^{3+} + Ho^{3+} crystals as room temperature laser in IR (3.9 μm) domain. The idea was to improve the pumping scheme of the initial laser level with sensitization of Ho^{3+} fluorescence by Tm^{3+} in BaF_2. They used low concentration RE doped BaF_2 (0.35÷1.3 at% HoF_3 and 0.3÷2.1 at% TmF_3). The Er^{3+} ions in fluoride crystals have spectroscopic properties that are favourable for cascade excitation (Kaminskii, 1996, 2007; Joubert et al., 1993). Er^{3+} ions doped BaF_2 crystals were investigated especially for upconversion luminescence (Johnson and Guggenheim, 1975; Patel et al., 1998; Wojtowicz and Wojtowicz., 2009,; Zhang et al., 2015; Bitam et al., 2018**).** Patel et. al. (Patel et al., 1998) demonstrated that, under excitation

at 805 nm, $BaF_2:Er^{3+}$ crystal is more efficient in generating red, green, and UV emissions than the $CaF_2:Er^{3+}$ crystal. Wojtowicz (Wojtowicz, 2009) studied the emissions under excitation in VUV spectral region. He identified a number of emission bands in VIS, UV and VUV. Zhang et al. (Zhang et al., 2015) detected very weak green and red emissions in Er^{3+} : BaF_2 crystals in comparison of the Er^{3+} doped $BaCl_2$ crystal when excited by 808 nm. Under 976 nm excitation, due to $^2H1_{1/2,}\ ^4S_{11/2} \rightarrow {}^4I_{15/2}$ transition, the green emission becomes dominant. The green luminescence, under excitation at 378 nm ($^4I_{15/2} \rightarrow {}^4G_{11/2}$ transition) was investigated by Bitam et. al. (Bitam et al., 2018) in BaF_2:2 mol% ErF_3. A very weak red emission (200 times weaker than the green emission), corresponding to the $^4F_{9/2} \rightarrow {}^4I_{15/2}$ transition, was reported. It has been proved that the use of radiation in UV range is an efficient tool for medical purposes such as the treatment of tissue, improving the phototherapy methods of some skin diseases, such as psoriasis, vitiligo or lymphoma (Vanó-Galván, 2012). Finding a laser material with emission in near UV range, for the construction of a solid, miniature laser, easy to manipulate by the patient itself is important.

Some radiation damages appear when the fluorides crystals are exposed to various radiations (x-rays, γ-rays, neutrons, etc). The radiation damage consists in appearance of new absorption bands caused by the color centers formation. These absorption bands reduce the transmission of the light through the crystal and change the optical properties of the crystals. Efforts have been made to find and understand the causes of the radiation damage. The presence of impurities and defects in crystal is the major reason for the radiation damage (Fedorov et al., 2016, Cooke and Bennett, 2003; Ren et al., 1994; Yin, 1994). Sabharwal et al. (2002), Shaoxia et al. (1994), Lingyan et al. (1994) and others also showed that the radiation damage is induced by oxygen and hydroxyl impurities in BaF_2 crystals. Ren et. al. (Ren et al., 1994), have investigated the effect of γ-rays on the optical properties of BaF_2 crystals grown under different vacuum level various conditions. They showed that new

optical absorption bands occur in the UV-VIS spectral domain after γ-rays irradiation due to presence of the oxygen ions. The radiation damage produced by a trace amount of Pb^{2+} ions in BaF_2 crystals was studied by Nicoara et al., (Nicoara et al., 2020). Rare-earth (RE) ions, such as Sm, Eu, Dy and Yb, which change its valence under irradiation, can eliminate the absorption bands of the color centers in the visible domain (Egranov and Sizova, 2013; Lingyan et al., 1994). There are few papers that analyze the influence of gamma radiation on the emission properties of the RE doped BaF_2 crystals, especially with Er^{3+} ions. We will mention only some of them. How the different impurities affect the radiation resistance of BaF_2 crystals is an open subject. Luo et al. (2016) studied the influence of Ce^{3+} ions in BaF_2 ceramic on the luminescence and scintillation properties. Two emissions with peak at 310 nm and 323 nm, when excited with both 279 nm and 300 nm, were observed. The radiation resistance of BaF_2:Ce^{3+} crystals and ceramics at gamma radiation was investigated by Fedorov et al. (2016). They reported the emission only for the unirradiated sample. Sizova et al. (2016) studied the optical absorption of x-rays irradiated Nd doped fluorides crystals. Yanagida et al., studied the emission and γ-rays responses of Nd:BaF_2 crystal; under 140-168 nm excitation the emission lines peaking around 180 nm, 230 nm and 260 nm.

The goal of this study is to investigate the influence of gamma-irradiation on the spectroscopic properties of the ErF_3 doped BaF_2 crystals for a low dopant concentrantion (0.2 mol% ErF_3). Many of the reported results about the emission are related to a high concentration of rare-earth ions in fluorides crystals. However, this study demonstrates a new UV luminescence at low Er^{3+} ions concentration in BaF_2 crystals, not reported before. The new UV luminescence can be related to the Er^{3+} isolated centers that predominates at low dopant concentration. The influence of Er3+ ions concentrations on the UV luminescence of BaF2:ErF3 is still under investigation. The Judd-Ofelt (J-O) analysis is performed in order to calculate the emission transition probabilities, branching-ratios and radiative lifetimes (Judd,

1962; Ofelt, 1962). The influence of gamma-rays doses on the J-O parameters and on the radiative lifetime is also investigated. To our knowledge, no other report of the influence of γ-rays on the emission spectrum of Er^{3+}-doped BaF_2 can be found in the literature.

2. Experimental

The ErF_3-doped BaF_2 crystal with a concentration of 0.2 mol% ErF_3 added to the melt was grown using the vertical Bridgman technique. The crystal was obtained in a spectral pure graphite crucible in vacuum (~0.1 Pa). The temperature distribution along the graphite heater and the corresponding used power during the heating and the cooling stages are shown in **Fig. 1a,b.** In order to obtain the temperature distribution, a shaped graphite heater was used (Nicoara and Nicoara, 1988). The temperature gradient, for a nominal power of 4.3 kW, is 35°C/cm (**Fig. 1c**). The pulling rate was ~4 mm/h. The obtained crystal is transparent, 6 cm in length and 1 cm in diameter. No visible inclusions were observed. The studied sample was cleaved from the middle of the crystal (**Fig. 1d**).

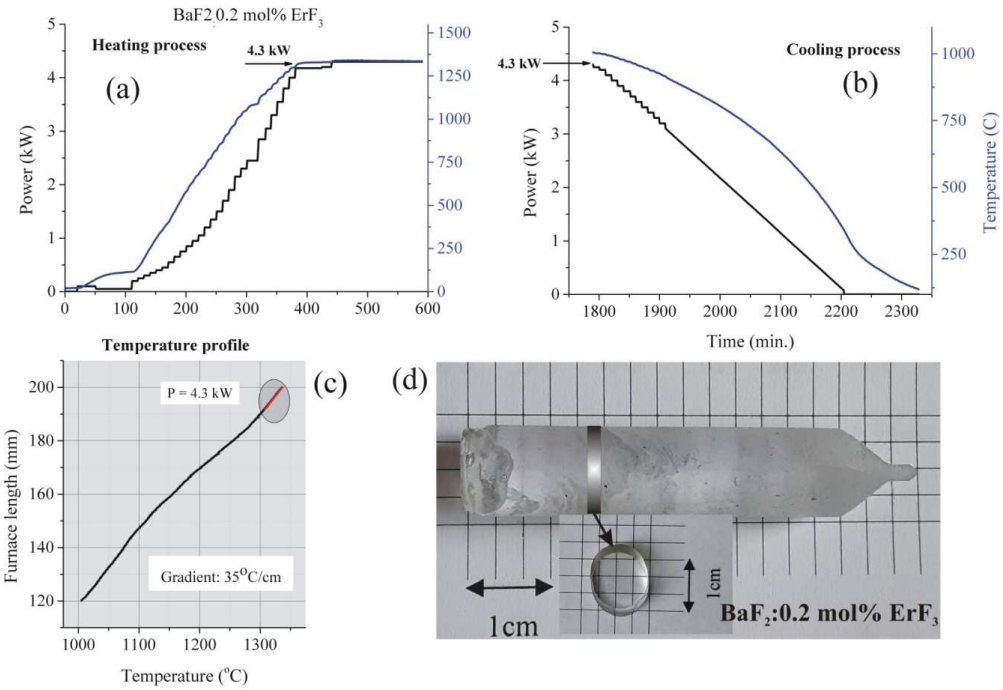

Fig. 1. Temperature distribution along the graphite heater and the corresponding used power: (a) during the heating stage and (b) during the cooling stage. (c) Temperature profile in the heater during the growth process. (d) BaF_2:0.2 mol% ErF_3 crystal and the cleaved sample.

Room temperature optical absorption spectrum, in UV-VIS domain, was recorded using a Shimadzu 1650PC spectrophotometer. IR absorption spectrum was obtained with a Nexus 470 FTIR spectrophotometer. Room temperature UV-VIS luminescence spectra and time resolved mesurements were recorded on FLS 980–Edinburgh Instruments spectrofluorimeter using Xe lamp as excitation source and scan slit of 0.1 nm. The cleaved sample was irradiated with γ-rays from a ^{60}Co source with the average energy of 1.2 MeV, up to a dose of 270 kGy.

3. Results and discussions

3.1. Optical absorption spectra

The UV-VIS-IR absorption spectrum of the sample (2.83 mm thick) is shown in **Fig. 2.** The absorption bands used for the least-square fitting procedure are highlighted. These peaks correspond to the transitions from the ground state, $^4I_{15/2}$, to the excited states of Er^{3+} ions, specified in the figure. The absorption spectrum before and after gamma irradiation ranging

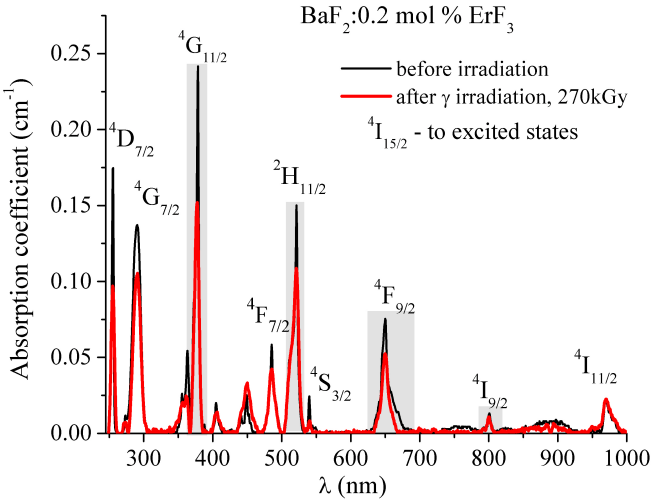

Fig. 2. Room temperature optical absorption spectrum of BaF_2:0.2 mol% ErF_3 crystal before and after γ-rays irradiation.

from 190 to 1000 nm consists of 12 absorption bands In order to preserve the electrical neutrality of the system, the trivalent erbium ion is compensated by a fluorine ion. The charge compensation is effected by interstitial fluorine ions in various positions relative to Er^{3+} ions, giving rise to various sites with cubic (O_h), tetragonal (C_{4v}) and trigonal (C_{3v}) site symmetries, the so-called isolated centers and various clusters (Petit et al., 2007). For low ErF_3 concentration (<0.1%), the so-called isolated centers predominate in the crystal. As the dopant concentration increases, besides of isolated centers additional complex defects, the clusters, are present in crystals. All these lead to a multisite structure of the absorption bands. Using laser selective excitation, Wells et al. (Wells et al., 2002) showed that the dominant isolated centre in lightly doped BaF_2:Er^{3+} crystals has C_{3v} symmetry, against the case of CaF_2:Er^{3+}, where the dominant centre is C_{4v}. The Gaussian multi-peaks decomposition reveals two major peaks in the case of the highlighted bands: at 372 nm and 378 nm, at 511nm and 521 nm, respectively at 640 nm and 649 nm. Taking into account the results of Tallant and Wright (Tallant and Wright, 1975) we attributed the 372 nm, 511 nm and 640 nm peaks to C_{3v} (*NNN*) site and the 378 nm, 521 nm and 649 nm peaks to clusters (aggregates). The strongest absorption bands are at ~ 254, 290, 378 and 520 nm, It is known that the presence of the impurities in crystal is the major reason for the radiation damage (Fedorov et al., 2016, Cooke and Bennett, 2003; Ren et al., 1994; Yin, 1994; Sabharwal et al., 2002; Shaoxia et al., 1994; Lingyan et al., 1994; Egranov and Sizova, 2013; Nicoara et al., 2020). The radiation damage is related to the appearance of the new absorption bands due to color center formation. Ren et al., (Ren et al., 1994) investigated the effects of various RE ions on the radiation damage of BaF_2. The elements which changes its valence from +3 to +4 under

irradiation are harmful, in contrast to the stable RE ions that have no effect on the radiation resistance of BaF_2.

No change in our OA spectrum was observed after irradiation, even at doses up to 270 kGy related to fact that no new absorption bands appeared after irradiation. Changes were observed related to the intensity of the every absorption bands. After irradiation, the intensity of the absorption bands decrease. Analyzing the absorption bands after irradiation, it was found that the intensity of the component corresponding to the clusters decrease. This means that after irradiation some of the clusters were "dissolved". Therefore, the areas corresponding to the OA bands are changed. The absorption line strengths for various transitions before and after γ-irradiation is calculate using the area of the band. This explain why differ the various JO parameters before and after irradiation.

3.2. Emission spectra

The room temperature emission spectra (**Fig. 3a,b**) was obtained by excitation under two intense bands: at $\lambda_{exc.}$=378 nm ($^4I_{15/2} \rightarrow {}^4G_{11/2}$ transition) and $\lambda_{exc.}$= 290 nm ($^4I_{15/2} \rightarrow {}^4G_{7/2}$ transition). The emission spectra before and after irradiation are shown in **Fig. 3a,b.**

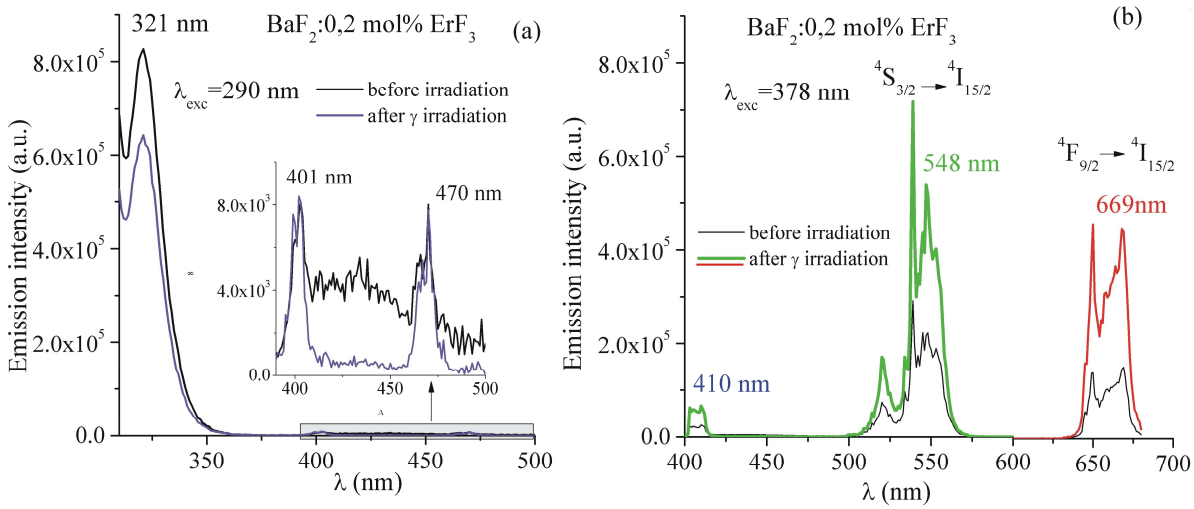

Fig. 3. Room temperature emission spectra of BaF_2: 0.2 mol% ErF_3 crystal by excitation by: (a) $\lambda_{exc.}$=290 nm and (b) $\lambda_{exc.}$=378 nm.

The emission spectrum by excitation at 378 nm is characterized by three emission bands (**Fig.3b)** One blue band, centered at 410 nm, one green band, around 540 nm and a red band, around 650 nm. The blue emission is ten times weaker than the green emission. These emissions correspond to the transitions from $^2H_{9/2}$, $^4S_{3/2}$ and $^4F_{9/2}$ excited levels to the $^4I_{15/2}$ ground level. The green emission (548 nm) intensity increases twice and the red emission (669 nm) three times after γ irradiation. The blue, green and red emission bands in BaF_2 host have been reported by other authors. Zhang et al., (Zhang et al., 2015) reported intense blue emission (410 nm) and green-blue emission (496 nm) in $BaCl_2:Er^{3+}$ when excited by 808 nm and 976 nm, respectively, but the luminescence in $BaF_2:Er^{3+}$ is extremely weak. Bitam et. al. (Bitam et al., 2018) studied the luminescence in BaF_2:2 mol% ErF_3. Under excitation at 378 nm, green (551 nm) and red (652 nm) emissions were detected. The red emision is 200 times weaker than the green emission. The emission spectrum by excitation at 290 nm is characterized by three emission bands (**Fig.3a**): two weak emission at 410nm and 470 nm, and one strong UV emission at 321 nm. The highest intensity has the UV emission, at 321 nm; after irradiation the intensity of this emission decreases a little. The UV emission centered at 321 nm (**Fig. 3a**) occurred under excitation at 290 nm has not been reported before. The UV emission was also observed in CaF_2 crystal around 314 nm that corresponds to the $^4D_{5/2} \rightarrow {}^4I_{13/2}$ transition (Preda et al., 2009). The observed emissions by 290 nm and 378 nm excitation are showed in the energy level diagram (**Fig.4a,b**). The emissions by 290 nm excitations are assigned to $^2P_{3/2} \rightarrow {}^4I_{15/2}$ transition (321 nm), the emission around 402 and 470 nm, comes from the transition $^2P_{3/2} \rightarrow {}^4I_{13/2}$, respectively $^2K_{15/2} \rightarrow {}^4I_{13/2}$ (**Fig. 4a**). The emission bands obtained by 378 nm excitation correspond to the following transitions: : $^4F_{9/2} \rightarrow {}^4I_{15/2}$ (660 nm, red), $^4S_{3/2} \rightarrow {}^4I_{15/2}$ (551 nm, green) and $^2G(1)_{9/2} \rightarrow {}^4I_{15/2}$ (410 nm, violet) (**Fig. 4b**).

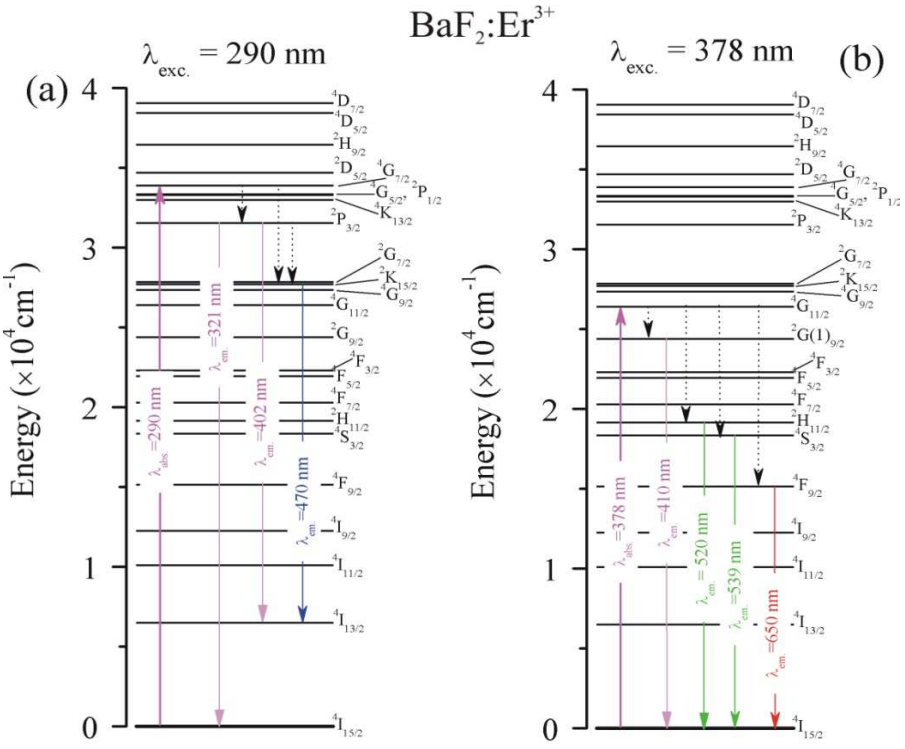

Fig. 4. The energy-level diagram of Er^{3+} ions under excitations (a) by 290 nm and (b) 378 nm.

3.3. Judd-Ofelt analysis

The behaviour of luminescence spectrum of ErF_3 doped BaF_2 crystal can be explained using the Judd-Ofelt model (Judd, 1962; Ofelt, 1962). The J-O intensity parameters (Ω_2, Ω_4, Ω_6) are used to evaluate the transition probabilities, the branching ratios and the radiative lifetime. These parameters are obtained using the best fit between the experimental absorption oscillator strengths and the theoretical ones. The J-O intensity parameters were calculated using a set of four absorption bands, highlighted in **Fig. 2**. These bands correspond to the transitions from $^4I_{15/2}$ ground state to $^4I_{9/2}$ (802 nm), $^4F_{9/2}$ (653 nm), $^2H(2)_{11/2}$ (519 nm) and $^4G_{11/2}$ (377 nm). In order to study the influence of gamma rays irradiation on the J-O spectroscopic parameters, the sample was irradiated at 70, 130 and 270 kGy

The experimental line strength, S_{meas}, has been evaluated from the absorption spectrum. And then was used to obtain the J–O parameters by solving simultaneously a set of four equations. In order to resolve this system of equations the Levenberg-Marquardt algorithm was used. The theoretical line strength $S_{\mathrm{calc}} = \mathrm{S}_{JJ'}^{\mathrm{ed}} + S_{JJ'}^{\mathrm{md}}$ is calculated using the obtained J-O parameters and the values of the reduced matrix elements for the chosen Er^{3+} bands from those tabulated in (Kaminskii, 1996). The measured and calculated absorption line strengths for transitions $^4I_{15/2} \rightarrow [^4I_{9/2}, {}^4F_{9/2}, {}^2H(2)_{11/2}, {}^4G_{11/2}]$, before and after gamma irradiation are shown in **Table 1.** A measure of the accuracy of the fit is given by the root-mean-square deviation, defined by: $\Delta S_{\mathrm{rms}} = [(q-p)^{-1}\sum(S_{\mathrm{calc}} - S_{\mathrm{meas}})^2]^{1/2}$, where q is the number of spectral bands analyzed (q = 4), and p is the number of the parameters sought (p = 3). The best root mean-square (r.m.s.) deviation between measured and calculated line strengths of the unirradiated sample are shown in **Table 1** for each transition.

Table 1. Measured and calculated absorption line strengths of Er^{3+}:BaF_2 crystal.

Transition $^4I_{15/2} \rightarrow$	λ_m [nm]	0 kGy		70 kGy		130 kGy		270 kGy	
		$S_{\mathrm{meas}}^{\mathrm{ed}}$	$S_{\mathrm{calc}}^{\mathrm{ed}}$	$S_{\mathrm{meas}}^{\mathrm{ed}}$	$S_{\mathrm{calc}}^{\mathrm{ed}}$	$S_{\mathrm{meas}}^{\mathrm{ed}}$	$S_{\mathrm{calc}}^{\mathrm{ed}}$	$S_{\mathrm{meas}}^{\mathrm{ed}}$	$S_{\mathrm{calc}}^{\mathrm{ed}}$
		(expressed in 10^{-20} cm^2)							
$^4I_{9/2}$	802	0.038	0.037	0.035	0.035	0.038	0.038	0.031	0.032
$^4F_{9/2}$	653	0.578	0.578	0.531	0.531	0.504	0.504	0.485	0.485
$^2H(2)_{11/2}$	519	0.76	0.826	0.745	0.737	0.750	0.742	0.779	0.763
$^4G_{11/2}$	377	1.113	1.062	0.940	0.947	0.947	0.953	0.967	0.980
	ΔS_{rms}:	0.084		0.011		0.010		0.021	

The obtained J-O parameters and the spectroscopic quality factor, $\chi=\Omega_4/\Omega_6$, are given in **Table 2.** A comparison of our J-O parameters to those obtained by other is also provided.

Table 2. Judd-Ofelt parameters and spectroscopic quality factors χ of Er^{3+} ions in the fluoride hosts.

Ω_t (10^{-20} cm^2)	BaF_2: 0.2 mol% Er^{3+} (This work)	BaF_2: 2 mol% Er^{3+} (Bitam et al., 2018)	BaF_2: 2 mol% Er^3 (Patel et al., 1998)	CaF_2: 2 mol% ErF_3 (Preda et al., 2009)
Ω_2	0.932	0.949	1.048	1.043
Ω_4	0.153	0.975	1.478	0.866
Ω_6	1.074	1.258	1.009	1.725
$\chi=\Omega_4/\Omega_6$	0.142	0.775	1.465	0.502

The influence of gamma irradiation dose on the J-O parameters is shown in **Table 3**; after irradiation the values of the J-O parameters decrease a little.

Table 3. The influence of gamma rays doses on the Judd-Ofelt parameters, Ω_t (10^{-20} cm^2) and the estimated error of the J-O parameters.

γ-dose (kGy):	0	70	130	270
Ω_2	0.932±0.84 (90%)	0.823±0.106 (12%)	0.827±0.104 (12%)	0.877±0.213 (24%)
Ω_4	0.153±0.06 (39%)	0.145±0.007 (5%)	0.169±0.007 (4%)	0.133±0.015 (11%)
Ω_6	1.074±0.13 (12%)	0.983±0.017 (2%)	0.897±0.017 (2%)	0.897±0.034 (4%)

The error of J-O parameters was estimated using the method described by (Görller-Walrand, 1998). These errors are not usually reported in the literature and therefore it is difficult to compare them. The main reason of the lack of this information in the literature could be related to the large error in the estimation of J-O parameters. In our case the errors varies between 2% and 90%. These large errors are not only due to inadequacies of the Judd-Ofelt theory, but also due to the difficulty of obtaining accurate absorption line strengths, especially in the case of overlapping bands. We calculated the spontaneous emission probabilities, $A_{JJ'}$, of the transitions to their corresponding lower-lying manifold states. The radiative lifetime τ_{rad} for an excited state J is calculated by $\tau_{rad} = 1/\sum A_{JJ'}$, where the sum is taken over all final lower-lying states J'. The fluorescence branching ratios, $\beta_{JJ'}$, can be calculated from the radiative decay rates and the radiative lifetimes using the relationship $\beta_{JJ'} = \tau_{rad} A_{JJ'}$, where the sum runs over all final states J'. The value of the radiative

emission probabilities, the radiative lifetimes and the branching ratios before and after gamma rays irradiation at the maximum dose are given in **Table 4**.

Table 4. The radiative emission probabilities, the lifetimes and the branching ratios, before and after gamma rays irradiation at the maximum dose.

Transitions	λ_{mean} [nm]	0 kGy			270 kGy		
		$A_{JJ'}$ (s^{-1})	β	τ_{rad} (ms)	$A_{JJ'}$ (s^{-1})	β	τ_{rad} (ms)
$^4I_{13/2} \rightarrow {}^4I_{15/2}$	1522	86.7	1	11.532	77.2	1	12.943
$^4I_{11/2} \rightarrow {}^4I_{15/2}$	976	72.7	0.89	12.277	61.1	0.89	14.609
$\rightarrow {}^4I_{13/2}$	2778	8.8	0.11		7.3	0.11	
$^4I_{9/2} \rightarrow {}^4I_{15/2}$	802	12.8	0.32	24.735	11.0	0.34	29.363
$\rightarrow {}^4I_{13/2}$	1739	27.3	0.68		22.8	0.36	
$\rightarrow {}^4I_{11/2}$	4651	0.3	~ 0		0.2	~0	
$^4F_{9/2} \rightarrow {}^4I_{15/2}$	653	380.1	0.9	2.297	319.0	0.88	2.727
$\rightarrow {}^4I_{13/2}$	1156	13.3	0.03		11.3	0.03	
$\rightarrow {}^4I_{11/2}$	1980	39.2	0.06		33.6	0.09	
$\rightarrow {}^4I_{9/2}$	3448	2.7	~ 0		2.7	~0	
$^4S_{3/2} \rightarrow {}^4I_{15/2}$	543	697.4	0.67	0.962	581.9	0.67	1.152
$\rightarrow {}^4I_{13/2}$	844	291.0	0.28		242.8	0.28	
$\rightarrow {}^4I_{11/2}$	1212	21.0	0.02		17.6	0.02	
$\rightarrow {}^4I_{9/2}$	1639.4	30.2	0.03		25.2	0.03	
$\rightarrow {}^4F_{9/2}$	3125	0.4	~ 0		0.3	~0	
$^2H(2)_{11/2} \rightarrow {}^4I_{15/2}$	519	921.9	0.89	0.958	850.5	0.88	1.037
$\rightarrow {}^4I_{13/2}$	791	75.0	0.07		71.3	0.07	
$\rightarrow {}^4I_{11/2}$	1105	17.1	0.02		15.8	0.02	
$\rightarrow {}^4I_{9/2}$	1449	26.6	0.02		23.4	0.02	
$\rightarrow {}^4F_{9/2}$	2500	3.5	~ 0		3.3	0.01	
$\rightarrow {}^4S_{3/2}$	12500	~ 0	~ 0		~0	~0	
$^4F_{7/2} \rightarrow {}^4I_{15/2}$	486	1384.6	0.90	0.647	1156.9	0.89	0.771
$\rightarrow {}^4I_{13/2}$	725	31.9	0.02		27.7	0.02	
$\rightarrow {}^4I_{11/2}$	980	51.5	0.03		43.4	0.03	
$\rightarrow {}^4I_{9/2}$	1242	68.4	0.04		58.7	0.05	
$\rightarrow {}^4F_{9/2}$	1942	9.8	~ 0		9.7	0.01	
$\rightarrow {}^4S_{3/2}$	5128	~ 0	~ 0		~0	~0	
$\rightarrow {}^2H(2)_{11/2}$	8696	~0.2	~ 0		0.1	~0	

The dependence of the calculated radiative lifetime on the gamma rays dose is shown in **Fig. 5.** The calculated radiative lifetimes corresponding to the observed emissions increase slightly with the gamma dose. The calculated and measured radiative lifetime, at various γ-rays doses (*D*) are given in **Table 5**.

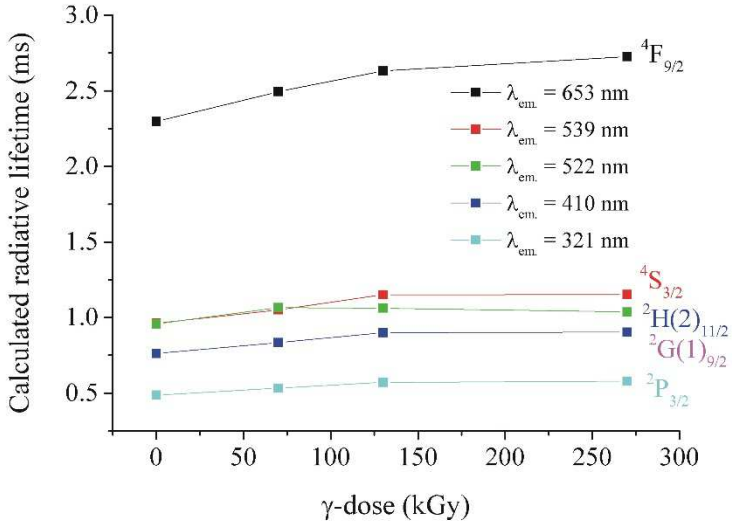

Fig. 5. Dependence of the calculated radiative lifetime on the gamma rays dose.

Table 5. The calculated and measured radiative lifetime of the transitions where luminescence were observed, at various γ-rays dose, *D*.

Energy level	$\lambda_{em.}$ nm	Calculated lifetime (ms) at various γ-rays doses, *D* (kGy)				Measured lifetime (ms)	
		D = 0	70	130	270	Before	after γ-irradiation
$^4F_{9/2}$	653	2.297	2.495	2.632	2.727	2.21	2.46 (This work) 0.95 (Bitam et al., 2018) 0.15(Deren and Mahiou, 2007)
$^4S_{3/2}$	539	0.962	1.051	1.151	1.152	1.138	1.005 (This work) 0.56 (Bitam et al., 2018) 0.88 (Patel et al., 1998) 0.39(Deren and Mahiou, 2007)
$^2H(2)_{11/2}$	522	0.958	1.066	1.062	1.037	0.04(Deren and Mahiou, 2007)	
$^2G(1)_{9/2}$	410	0.762	0.835	0.900	0.903	1.418 (Zhang et al., 2015)	
$^2P_{3/2}$	321	0.487	0.533	0.571	0.579	-	

Fig. 6 shows the decay curves of the ($^2H(2)_{11/2}$+$^4S_{3/2}$)→ $^4I_{15/2}$ transition (green emission) and of the $^4F_{9/2}$→ $^4I_{15/2}$ transition (red emission). The behavior of the both decay luminescence is nonexponetial. They have been fitted by a double exponential function which give an effective lifetime of 1.005 ms for the green emission and of 2.46 ms for the red emission for the irradiated sample. These values are in a good agreement with those calculated using J-O

formalism, but also with those obtained by other authors (**Table 5**) (Zhang et al., 2015; Bitam et al., 2018; Patel et al., 1998; Deren and Mahiou, 2007). The lifetime for the purple emission was not determined by the lack of equipment.

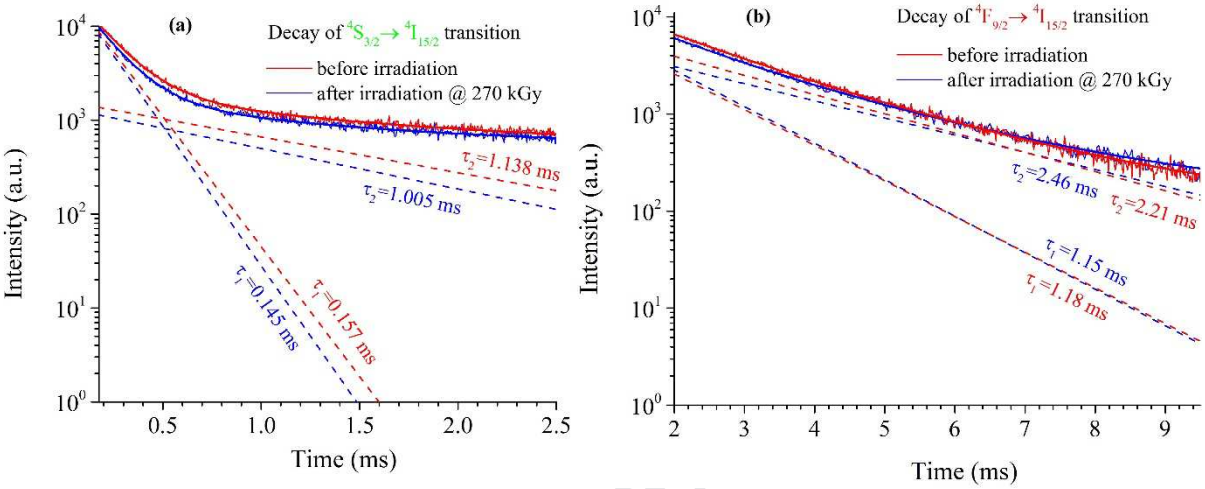

Fig. 6. The decay curves of the (a) ($^2H(2)_{11/2}$+$^4S_{3/2}$)→ $^4I_{15/2}$ transition (green emission) and (b) of the $^4F_{9/2}$→ $^4I_{15/2}$ transition (red emission) before and after γ-rays irradiation.

The emission cross section corresponding to the observed emission was estimated using Füchtbauer-Ladenburg expression (Deren and Mahiou, 2007):

$$\sigma_{em}(\lambda) = \frac{\lambda^5 I(\lambda)}{8\pi[n(\lambda)]^2 c\tau_{\mathrm{rad}} \int \lambda I(\lambda)\mathrm{d}\lambda}$$

where $I(\lambda)$ is the emission intensity at each wavelength, τ_{rad} is the radiative lifetime of the upper laser level and β is the branching ratio, n is the refractive index and c is the velocity of light. The emission cross section of the purple, green and red emission spectra of BaF_2:0.2 mol% ErF_3 sample before and after γ-rays irradiation is shown in **Fig. 7**. The optical gain parameter for the main emission bands is also shown in the figures.

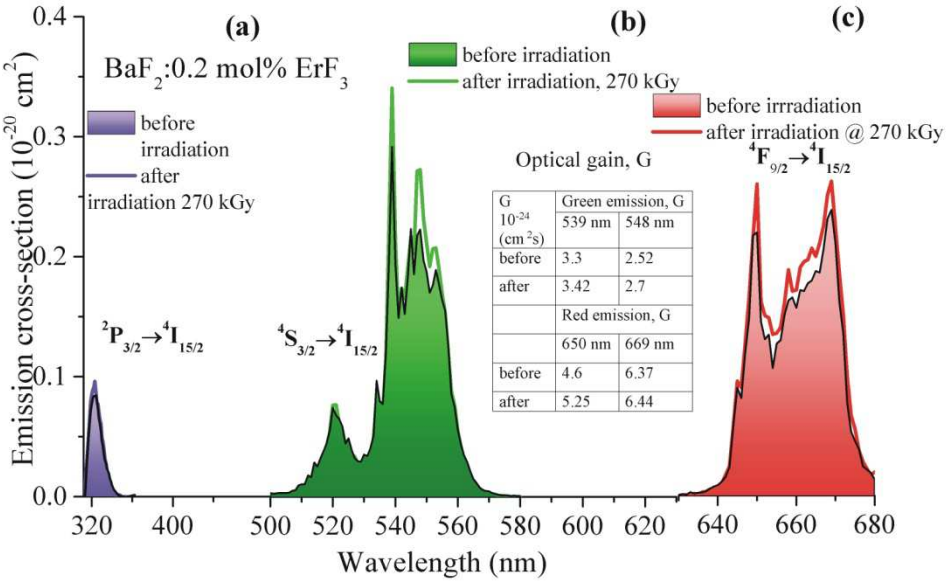

Fig. 7. Emission cross section of BaF_2:0.2 mol% ErF_3 crystal for (a) the violet, (b) the green and (c) the red luminescence. The optical gain parameter is also shown.

The optical gain parameter, defined as $G = \sigma_{em}\tau_{exp}$, is an important parameter in order to evaluate the laser performance of the material. The optical gain parameter The optical gain parameter, of the irradiated sample, is 3.42×10^{-24} $cm^2\cdot s$ for green emission and 6.44×10^{-24} $cm^2\cdot s$ for red emission. The optical gain parameter increases slightly with the gamma dose. Therefore, the red emission is more attractive than the green emission for laser applications.

4. Conclusions

The influence of gamma rays irradiation on the optical absorption and luminescence of the ErF_3 doped BaF_2 crystals for a low dopant concentrantion (0.2 mol% ErF_3) was investigated. The Judd-Ofelt analysis is performed in order to calculate the emission transition probabilities, the branching-ratios, the radiative lifetimes and the gain parameter for green and red emissions. The values of the J-O parameters are slightly influenced by gamma rays irradiation, even at maximum dose of 270 kGy. The calculated radiative lifetimes increase slightly with increasing the gamma rays dose. The measured lifetimes of the irradiated

sample for the green and the red emissions are 1.005, respectively 2.46 ms. These values are in a good agreement with those calculated using the J-O formalism. Apart from the green and red emissions, arising under excitation by 378 nm, a new, intense UV emission band, centered at 321 nm (corresponding to the $^2P_{3/2} \rightarrow {}^4I_{15/2}$ transition) was observed under excitation by 290 nm. This emission was not reported before. The energy-level diagram of the excitation and emission mechanism was proposed. The optical gain parameter increases slightly with the gamma dose. The optical gain parameter resulted from this study is 3.3×10^{-24} $cm^2 \cdot s$ for the green emission and 6.4×10^{-24} $cm^2 \cdot s$ for the red emission. Therefore, the red emission of BaF_2:0.2 mol% ErF_3 crystal is more attractive for laser applications than the green emission.

Acknowledgment

This work was supported by a grant of the Romanian Minister of Research and Innovation, PCCDI-UEFISCDI, project number PN-III-P1-1.2-PCCDI-2017-0152/75PCCDI/2018 within the project PNCDI III. Authors are thankful to PhD Constantin Daniel Negut for gamma-rays irradiations.

References

Bitam, A., Khiari, S., Diaf, M., Boubekri, H., Boulma, E., Bensalem, C., Guerbous, L. Jouart, J.P., 2018. Spectroscopic investigation of Er^{3+} doped BaF_2 single crystal. Opt. Mater. 82, 104-109.

Cooke, D.W., Bennett, B.L., 2003. Optical absorption and luminescence of 14-MeV neutron-irradiated CaF_2 single crystals. J. Nucl. Mater. 321, 158–164.

Egranov, A.V., Sizova, T.Yu., 2013. Configurational instability at the excited impurity ions in alkaline earth fluorites. J. Phys. Chem. Solids 74, 530–534.

Deren, P.J., Mahiou, R., 2007. Spectroscopic characterisation of $LaAlO_3$ crystals doped with Er^{3+} ions, Opt. Mater. 29, 766-772.

Fedorov, P.P., Ashurov, M.Kh., Boboyarova, Sh.G., Boibobeva, S., Nuritdinov, L., Garibind, E.A., Kuznetsova, S.V., Smirnove, A.N., 2016 Absorption and luminescence spectra of CeF_3 doped BaF_2 single crystals and nanoceramics. Inorg. Mater. 52, 213–217.

Görller-Walrand C., Binnemans K., 1998. Spectral intensities of f-f transitions. Handbook on the Physics and Chemistry of Rare Earths, 25, USA: Elsevier Science B.V, p.167

Hahn, D., 2014. Calcium fluoride and barium fluoride crystals in optics. Optik&Photonik 9, 45-48.

Johnson, L.F., Guggenheim, H.J., 1975. Infrared-pumped visible laser. Appl. Phys. Lett. 19, 44-47.

Joubert, M.F., Guy, S., Jacquier, B., 1993. Model of the photon-avalanche effect. Phys. Rev. B 48, 10031-10037.

Judd, B.R., 1962. Optical absorption intensities of rare-earth ions. Phys. Rev. 127, 750-761.

Kaminskii, A., 2007. Laser crystals and ceramics: recent advances. Laser Photonics Rev. 1, 93-177.

Kaminskii, A.A., 1996. Crystalline Lasers: Physical Processes and Operating Schemes. Boca Raton, FL: CRC Press.

Luo J., Sahi S., Groza M., Wang Z., Ma L., Chen W., Burger A.. Kenarangui R., Sham T.-K., Selim F.A., 2016. Luminescence and scintillation properties of BaF_2-Ce transparent ceramic. Opt. Mater. 58, 353-356.

Lingyan C., Mu. G., Jie C., Kaihua D., Gang X., Shaoxia C., Fengyin R., 1994. The radiation effect mechanism of some rare earth doped BaF_2 crystal. Mat. Res. Soc. Symp. Proc. 348, 441-446.

Nicoara, D., Nicoara, I., 1988. An improved Bridgman-Stockbarger crystal-grown system. Mater. Sci. Eng. A 102, L1-L5.

Nicoara, I. , Stef, M., 2016. Charge compensating defects study of YbF_3-doped BaF_2 crystals using dielectric loss. Phys. Status Solidi B 253, 397-403.

Nicoara, I., Stef, M., Vizman, D., 2020. Influence of Pb^{2+} ions on the optical properies of gamma irradiated BaF_2 crystals. Radiat. Phys. Chem. 168, 108565.

Ofelt, G.*S.*, *1962*. Intensities of crystal spectra of rare-earth ions. J. Chem. Phys. 37, 511-520.

Orlovskii Yu.V, Basiev T.T., Pukhov K.K., Alimov O.K., Glushkov N.A., Konyushkin V.A.,2010. Low-phonon BaF_2: Ho3+, Tm3+ doped crystals for 3.5–4 μm lasing. Opt. Mater. 32, 599–611.

Patel, D.N., Reddy, R.B., Nash-Stevenson, S.K., 1998. Diode-pumped violet energy upconversion in BaF_2:Er^{3+}. Appl. Opt. 33, 7805-7808.

Petit V., Camy P., Doualan J.L., Moncorge R., 2007. Refined analysis of the luminescent centers in the Yb^{3+}:CaF_2 laser crystal, J. Lumin. 122-123, 5-7.

Preda, E., Stef, M., Buse, G., Pruna, A., Nicoara, I., 2009. Concentration dependence of the Judd–Ofelt parameters of Er^{3+} ions in CaF_2 crystals. Phys. Scr. 79, 035304.

Ranon U., Yaniv A., 1964. Charge compensation by interstitial F^- ions in rare-earth doped SrF_2 and BaF_2. Phys. Lett. 9, 17-19.

Ren, S., Chen, G., Zhang, F., Zheng, Y., 1994. The effect of impurities on the radiation damage of barium fluoride crystal. Mat. Res. Soc. Symp. Proc. 348, 435-440.

Sabharwal, S.C., Sangeeta, H.P., Chauhan, A.K., 2002, Effect of lattice oxygen on optical absorption, radiation hardness and thermally stimulated luminescence of BaF_2 crystal, J. Cryst. Growth 240, 473-478.

Shaoxia, R., Chen, G., Zhang, F., 1994. Scintilator and phosphor materials. Mater. Res. Soc. Symp. Proc., 348, 105-110.

Sizova, T., Radzhabov, E., Shendrik, R., Egranov, A., Shalaev, A., 2016. Study of Nd^{2+} absorption in x-irradiated CaF_2, SrF_2, BaF_2 crystals. Rad. Meas. 90, 68-70.

Tallant D.R., Wright J. C., 1975. Selective laser excitation of charge compensated sites in CaF_2:Er^{3+}, J. Chem. Phys., 63, 2074-2085.

Vanó-Galván, S., Gárate, M.T., Fleta-Asín, B., Hidalgo, Á., Fernández-Guarino, M., Bermejo, T., Jaén, P., 2012. Analysis of the cost effectiveness of home-based phototherapy with narrow-band UV-B radiation compared with biological drugs for the treatment of moderate to severe psoriasis. Actas Dermosifiliogr. 103, 127-137.

Wells J.-P. R, Dean T., Reeves R. J., 2002. Site selective spectroscopy of the C_{3v} symmetry centre in Er^{3+} doped BaF_2. J. Lumin. 96, 239-248.

Wojtowicz, A.J., 2009. VUV spectroscopy of BaF_2:Er. Opt. Mater. 31, 474-478.

Witkowski M.E., Wojtowicz A.J.**,** 2011. High and low spin energy states of the Tb^{3+} $4f^7$5d configuration in BaF_2. Opt. Mater. 33, 1535-1539.

Yanagida, T., Kawaguchi, N., Yokota, Y., Ishidu, S., Fukuda, K., Yoshikawa, A., Pejchal, J., Nikl, M., Babin, V., Sekiya, H., Kamada, K., 2010. Study of VUV emission and γ-ray responses of Nd:BaF_2 scintillator. Rad. Meas. 45, 422–425.

Yin, Z.W., 1994. Research and development works on BaF_2 crystals in Shanghai Institute of ceramics. Mat. Res. Soc. Symp. Proc. 348, 65-76.

Zhang X., Chen Z., Qiu J., 2015. Mechanistic investigation of upconversion luminescence in Er^{3+}-doped $BaCl_2$, BaF_2 and $NaYF_4$ phosphors. Mater. Chem. Phys. 162, 76-81.

H I G H L I G H T S

- Good quality BaF_2:0.2 mol% ErF_3 crystal was grown by Bridgman method.
- Gamma rays effects were investigated by optical absorption studies.
- The influence of gamma rays on the Judd-Ofelt spectroscopic parameters was investigated
- New UV emission band arround 321 nm was observed under excitation at 290 nm.
- The calculated radiative lifetimes increase slightly with the gamma dose.

Declaration of interests

The authors declare that they have no known competing financial interests or personal relationships that could have appeared to influence the work reported in this paper.